



Science Arts & Métiers (SAM)

is an open access repository that collects the work of Arts et Métiers ParisTech researchers and makes it freely available over the web where possible.

This is an author-deposited version published in: <https://sam.ensam.eu>
Handle ID: <http://hdl.handle.net/10985/18719>

To cite this version :

Faissal CHEGDANI, Mohamed EL MANSORI, Satish T.S. BUKKAPATNAM, Iskander EL AMRI -
Thermal effect on the tribo-mechanical behavior of natural fiber composites at micro-scale -
Tribology International - Vol. 150, p.1-7 - 2019

Any correspondence concerning this service should be sent to the repository

Administrator : archiveouverte@ensam.eu



Thermal effect on the tribo-mechanical behavior of natural fiber composites at micro-scale

Faissal Chegdani^{a,b,*}, Mohamed El Mansori^{a,b}, Satish T.S. Bukkapatnam^a, Iskander El Amri^a

^a Texas A&M University, Department of Industrial and Systems Engineering, 3131 TAMU, College Station, TX, 77843, USA

^b Arts et Métiers ParisTech, MSMP Laboratory / EA7350, Rue Saint Dominique BP508, Châlons-en-Champagne, 51006, France

ABSTRACT

Keywords:

Natural fiber composites
Nanoindentation
Scratch
Friction

This paper aims to explore the thermal influence on the micro-tribo-mechanical behavior of natural fiber composites. Nanoindentation and scratch-test are used to characterize flax fibers reinforced polypropylene (PP) composites. Results show a different thermo-mechanical behavior between flax fibers and PP matrix. While the stiffness of PP matrix decreases by increasing the sample temperature, the stiffness of flax fibers shows an increase then a decrease by changing the sample temperature from 25 °C to 100 °C with a maximum at 60 °C. This attests to a modification of the chemical composition of flax fibers when increasing the temperature. The specific thermo-mechanical behavior of flax fibers affects their friction comportment at a high sliding speed which demonstrates that the tribology of NFRP composites is thermo-mechanical-dependent.

1. Introduction

In the context of the circular economy and sustainable development, the industry increasingly seeks eco-friendly material to meet the environmental standards [1–6]. Therefore, natural fiber reinforced polymer (NFRP) composites are emerging as a competitor to the traditional synthetic glass fiber composites materials in the automotive and aerospace industries thanks to their efficient mechanical properties [3,7]. Moreover, natural fibers show pertinent tribological performances with NFRP composites by increasing the wear resistance and reducing the friction coefficient during tribological solicitations [8–13].

Machining processes of NFRP composites have attracted industrial as well as academic research because these materials require some machining operations to achieve the finalized product. This is particularly so for long fiber composites because of the periphery burrs after the thermocompression operation [14,15]. Nevertheless, machining processes mechanics for NFRP composites is still not well mastered because of the complex cellulosic structure that characterizes natural fibers [16]. Moreover, the machinability analysis of NFRP composites requires the consideration of an appropriate analysis scale. The pertinent analysis scale for NFRP machining is related to the natural fibrous reinforcement size [17–21] because the tribo-mechanical response of natural fibers inside composite materials is strongly dependent on the contact scale [22–24]. However, the machining processes are not purely based on tribo-mechanical phenomena since the machining operations

induce significant temperature increase due to the high deformation rate and high tool/material friction [25,26]. Therefore, the induced thermal effect must be considered because the machining tribo-system of NFRP composites could be thermo-mechanical dependent.

Thermo-mechanical investigation of the tribological behavior of NFRP composites is really complicated during the machining process, especially when micro-analysis scales are required for this kind of complex materials because the mechanical properties of natural fibers show a scale effect (which is not the case for the PP matrix) [22,23]. Therefore, the thermo-mechanical data capture and processing in the case of NFRP machining must be made by a specific tribo-mechanical approach that allows the reproduction of the cutting contact tribology at micro-scale, which corresponds to the contact scale between the elementary flax fiber and the cutting edge radius. Thus, nanoindentation and scratch-test techniques can address this issue since the mechanical contact generated by these two methods can be extrapolated to the machining contact behavior between the cutting tool edge and the elementary flax fibers at the beginning of the cutting engagement [22,23].

In this paper, nanoindentation and scratch-test experiments are performed on flax fibers reinforced polypropylene (PP) composites at different sample temperatures (ranging from 25 °C to 100 °C). The thermo-mechanical data from nanoindentation and scratch-test are captured and processed in order to get both the Young's modulus and the dynamic friction coefficient at micro-scale. This will allow

* Corresponding author. Texas A&M University, Department of Industrial and Systems Engineering, 3131 TAMU, College Station, TX, 77843, USA.

E-mail address: faissal.chegdani@ensam.eu (F. Chegdani).

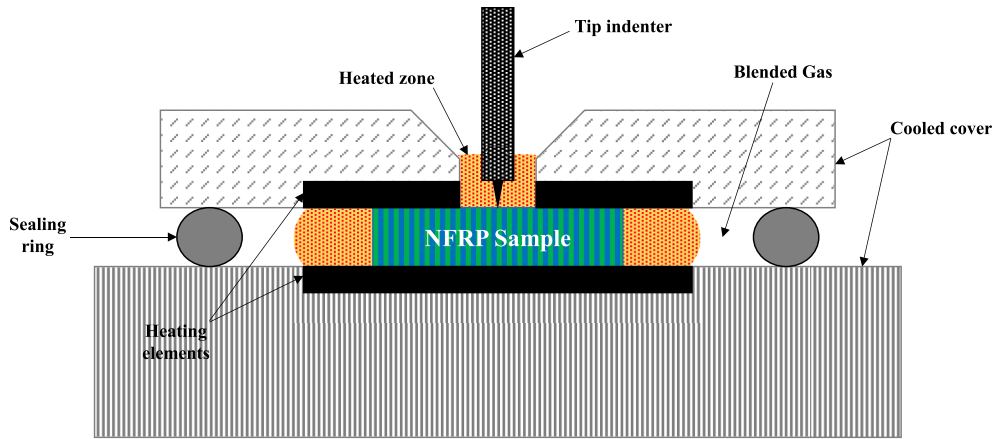


Fig. 1. Schematic depiction of the thermal setup in TI-950 Triboindenter.

investigating the tribological behavior of fibers and matrix separately.

2. Experimental procedure

Nanoindentation and scratch-test experiments are performed on Hysitron TI-950 Triboindenter. The thermal control is achieved using Hysitron “xSol800” high-temperature stage integrated into the triboindenter [27]. Fig. 1 illustrates the setup of this heating device. The NFRP workpiece is placed between two resistive heating elements that produce a uniform heated zone isolated by a thermal shield made from a low thermal capacity material. The heat transfer to the NFRP workpiece is assured by thermal conduction between the sample and the heating element in the micro-environment. With a small sample volume ($10 \times 4 \times 1$ mm), the thermal equilibrium is instantaneously reached. Thus, the temperature tracking is made by thermocouples placed on the heating elements. The tip indenter reaches the same temperature of the sample and the heating elements since it is located in the heated zone. The heat transfer to the tip indenter is assured by convection of the gas flow and radiation.

NFRP workpieces (Fig. 2(a)) are composites of unidirectional flax fibers (40% vt) embedded in a polymer matrix of polypropylene (60% vt). The worksurface is taken perpendicular to the fiber orientation in order to work on the fibers cross-sections as shown in Fig. 2(b). In this figure, flax fibers show a random shape, random diameter, and random distribution. Flax fibers are either presented as elementary fibers or as technical fibers (i.e. bundle of elementary fibers). The considered NFRP samples are manufactured and supplied by “Composites Evolution – UK”. More technical data about the NFRP samples in Ref. [21]. All the NFRP worksurfaces are polished with the same grit size ($\sim 3 \mu\text{m}$) in the same conditions to have identical initial surface states.

The tip indenter used in this study is a Hysitron Sapphire xSol probe on polycarbonate (ref. AA06031502) which is pyramidal Berkovich

probe designed for high temperature use. The tip radius is 150 nm. The tip calibration is performed on a fused quartz sample to obtain the contact area function.

During the nanoindentation experiments, a progressive force is applied toward the tip indenter after its engagement on the worksurface to reach a maximum value (F_{max}) that allows the tip indenter to penetrate the material (i.e. flax fiber or polypropylene matrix) as shown in Fig. 3(a). Penetration and withdrawal actions of the tip indenter generate a loading-unloading curve that can be used to calculate the Young's modulus of the indented material as explained in details in our previous work [22,23].

During the scratch-test experiments, the scratching length is chosen as $10 \mu\text{m}$ to work on fibers cross-sections and matrix separately. The tip is first engaged in the middle of the scratching line. Then, the tip is moved to one extremity of the cutting line before applying a maximum load of $500 \mu\text{N}$ as illustrated in Fig. 3(b). The scratching occurs by moving the tip to the other extremity of the scratching line with a constant applied load. The scratching time (Δt in Fig. 3(b)) is controlled to modify the sliding speed. The friction coefficient is thus calculated as the ratio between the friction force and the normal force.

3. Results and discussion

3.1. Thermal effect on NFRP mechanical behavior

Fig. 4 shows flax fiber cross-sections after indentation. At the same applied load, the indentation traces are more obvious at room temperature and becomes less visible when increasing the sample temperature. On the other side, the indentation traces of polypropylene matrix become more obvious by increasing the sample temperature as shown in Fig. 5. By measuring the indentation size after scanning (ΔD in Figs. 4 and 5), it can be seen that the indentation size on polypropylene

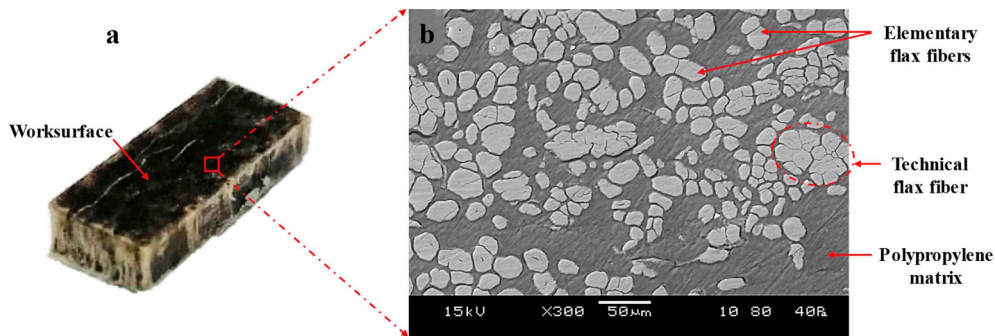


Fig. 2. (a) photograph of the NFRP sample. (b) Scanning Electron Microscope image of the NFRP worksurface showing the elementary fibers, the technical fibers, and the PP matrix.

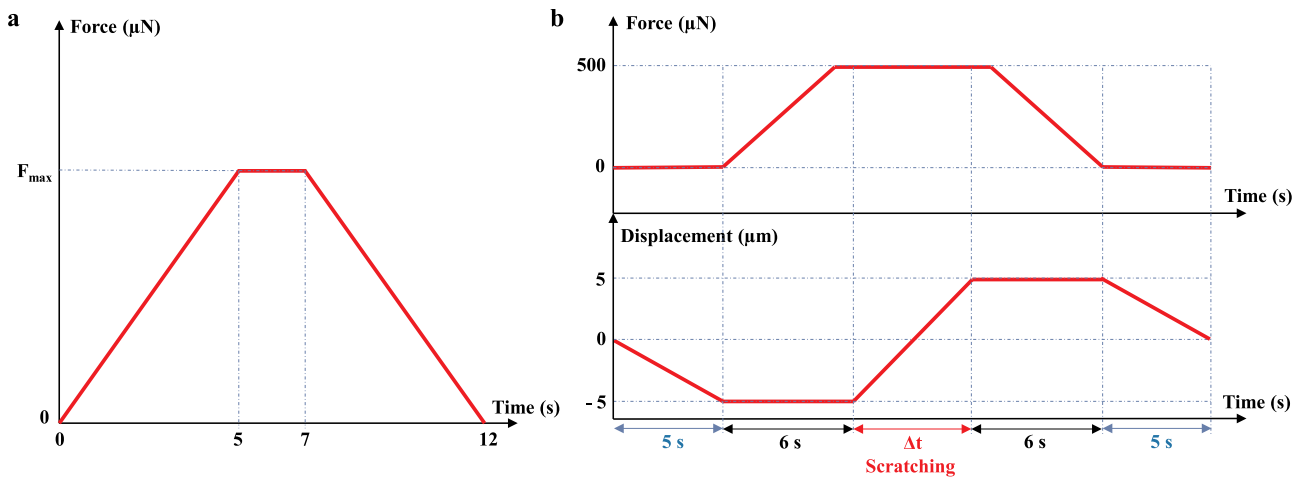


Fig. 3. (a) Load function for nanoindentation experiments. (b) Load function/tip displacement for scratch-test experiments.

matrix increases significantly by temperature increase at the considered thermal range, while the indentation size on flax fiber cross-sections decreases by temperature increase up to 60 °C. Above 60 °C, the indentation size on flax fibers does not show an important variation. Therefore, flax fibers and polymer matrix do not have the same indentation response as the temperature is varied.

Fig. 6 illustrates the loading-unloading curves acquired from the indentation experiments. Unlike the polypropylene matrix where the contact depth increases by increasing the sample temperature (Fig. 6(b)), flax fibers show a specific thermal behavior in terms of contact depth of the tip indenter (Fig. 6(a)). Indeed, for flax fiber cross-sections, the contact depth decreases with the sample temperature increase until reaching 60 °C. Then, beyond a sample temperature of 60 °C, the contact depth starts to increase with temperature rise to be equivalent or slightly greater than the contact depth values at room temperature (25 °C). This is a sign that the thermo-mechanical response of flax fibers is different from that of polypropylene matrix. Investigating the Young's modulus behavior of the two materials under the considered thermal conditions should qualitatively validate this hypothesis.

Fig. 7 presents the Young's modulus behavior of polypropylene matrix in function of the applied sample temperature. It can be seen that increasing the sample temperature decreases significantly the stiffness of PP matrix (Fig. 7(b)). Moreover, increasing the sample temperature increases the indentation contact depth at identical applied load (Fig. 7(a)). This shows that the temperature affects strongly the softening of PP matrix. On the other side, the thermal effect on flax fibers is completely different as shown in Fig. 8. Indeed, in the

temperature range of [25–60 °C], the Young's modulus of flax fibers increases by temperature increase. However, in the temperature range of [60–100 °C], the Young's modulus of flax fibers decreases by temperature increase.

The thermo-mechanical behavior of PP matrix shown in Fig. 7 is well known in the literature as a thermoplastic polymer [28,29]. Moreover, the thermo-mechanical effect is more obvious on PP matrix because its glass transition temperature (T_g) is much lower than the ambient temperature (between –23 and –10 °C) [30]. Thermoplastic matrices soften under the effect of heat and become malleable at high temperatures with a significant decrease of the viscosity [31].

The specific behavior of flax fibers under thermal nanoindentation may be due to the chemical composition of their cellulosic structure. Indeed, natural fibers are composed of a stack of cell walls with a central channel called lumen which is responsible for water and nutrient transportation [32] (Fig. 9). Each cell wall is itself a composite structure of cellulose microfibrils embedded in natural amorphous polymers of hemicellulose and lignin. In addition to this chemical composition, water molecules are added because all natural fibers are hydrophilic and tend to absorb moisture from the environment [33]. Therefore, when indenting flax fibers from 25 °C to 60 °C, increasing temperatures lead to water release which is acting as a plasticizer into the fiber structure [34]. This thermal effect on moisture content of flax fibers can explain the stiffness increase when heating flax fibers in the temperature range [25 °C–60 °C]. Above 60 °C, glass transition temperatures of the amorphous polymers inside the flax fiber are reached which make the fiber softer. Concretely, the glass transition temperature is 40 °C for hemicelluloses, 50 °C–100 °C for lignin, and above

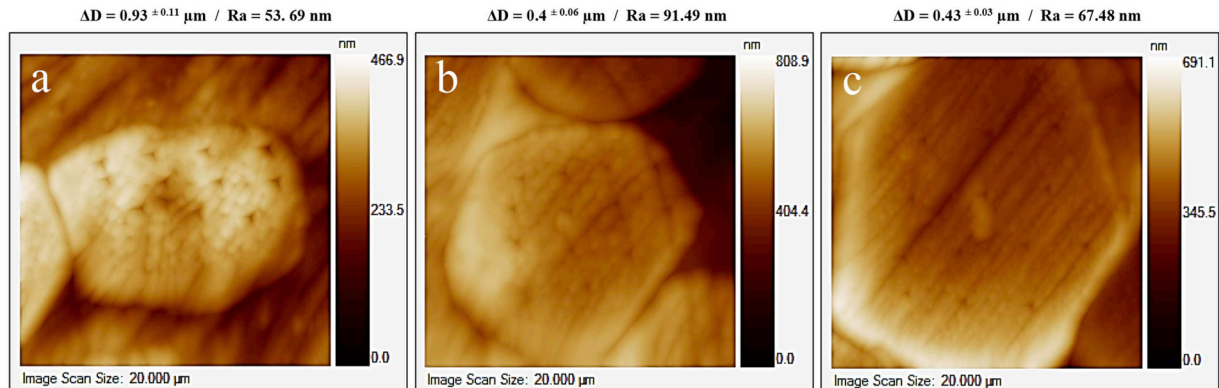


Fig. 4. Typical scanning probe image of flax fiber cross section after indentation with 500 μN of applied load showing the indentation size (ΔD) and the average surface roughness (R_a). (a) at 25 °C, (b) at 60 °C and (c) at 100 °C.

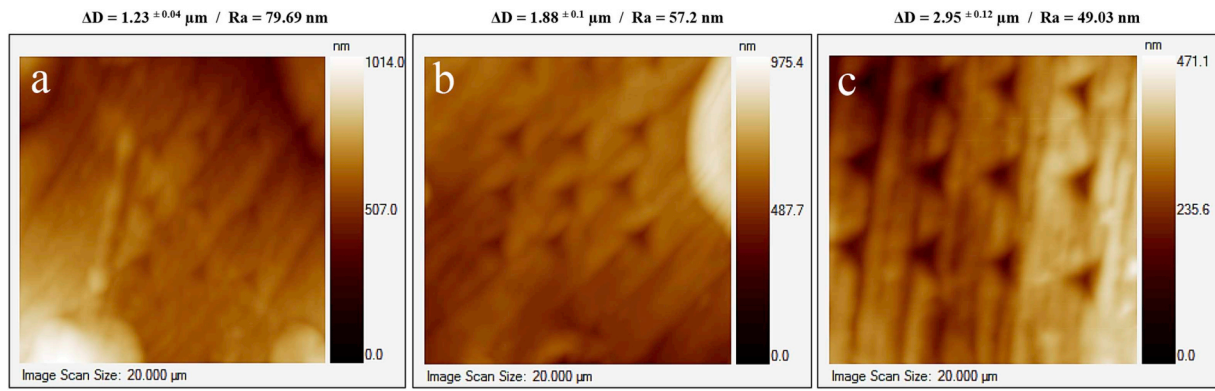


Fig. 5. Typical scanning probe image of polypropylene matrix after indentation with 500 μN of applied load showing the indentation size (ΔD) and the average surface roughness (R_a). (a) at 25 $^{\circ}\text{C}$, (b) at 60 $^{\circ}\text{C}$ and (c) at 100 $^{\circ}\text{C}$.

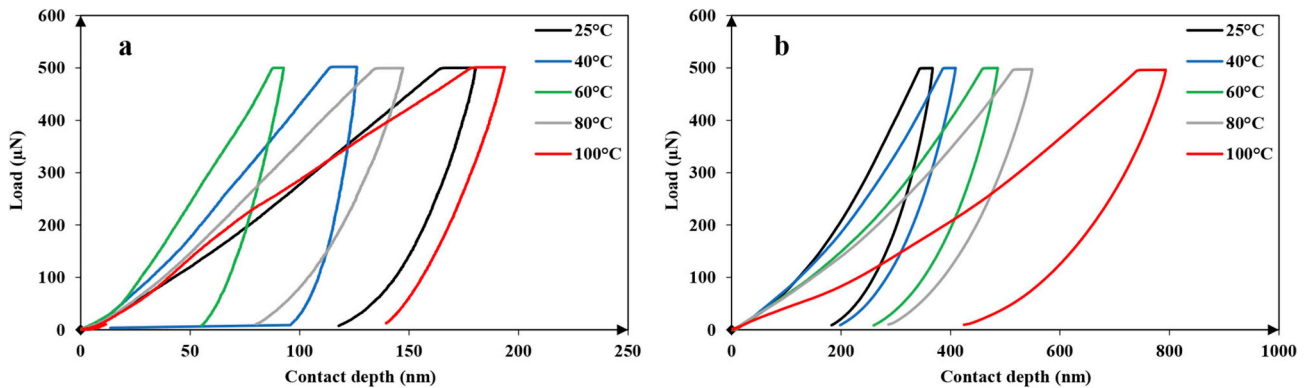


Fig. 6. Typical nanoindentation curves with 500 μN of applied load for (a) flax fibers and (b) polypropylene matrix.

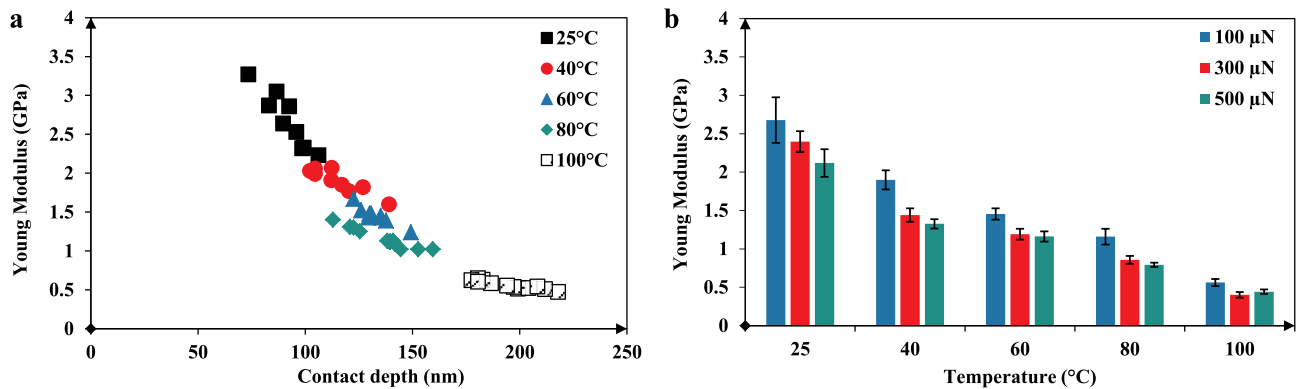


Fig. 7. Young's Modulus values obtained from nanoindentation of Polypropylene matrix at different sample temperatures, (a) with 500 μN of applied load, and (b) for different applied load values.

100 $^{\circ}\text{C}$ for cellulose [35]. Therefore, increasing the temperature above 60 $^{\circ}\text{C}$ leads to exceeding the T_g of lignin which is responsible for the rigidity of the cell wall as shown in Fig. 9 and, consequently, the rigidity of fiber decreases when heating flax fibers in the temperature range [60 $^{\circ}\text{C}$ –100 $^{\circ}\text{C}$].

3.2. Thermal effect on NFRP friction behavior

Fig. 10 presents typical scratching grooves with 10 μm of length for both flax fiber and PP matrix at different temperatures with different identified regimes. For flax fibers, the only regime is a region of rubbing and plowing with no chip formation. The traces depths of flax groove are deeper and larger at 25 $^{\circ}\text{C}$ and 100 $^{\circ}\text{C}$ than at 60 $^{\circ}\text{C}$. This observation corresponds to the mechanical response obtained with flax indentation

because the elastic modulus of flax fibers shows its highest value at 60 $^{\circ}\text{C}$ (Fig. 8) which leads to have the lowest plastic deformation when scratching. For PP matrix, two regimes are identified whatever the tested temperature. The first of these is a region of rubbing and plowing with no chip formation where the scratching traces are roughly parallel to the longitudinal scratching direction. The second region is where the transition occurs with chip formation initiation and a transverse trace starts to appear. Since the scratching length is low (10 μm), the scratching depth has not reach the minimum critical value to start an effective chip formation.

Fig. 11 illustrates the friction coefficient resulted from scratch test experiments on flax fibers and PP matrix separately. Globally, PP matrix generates lower friction than flax fibers. For the PP matrix, the friction coefficient decreases with temperature increase and it is not affected by

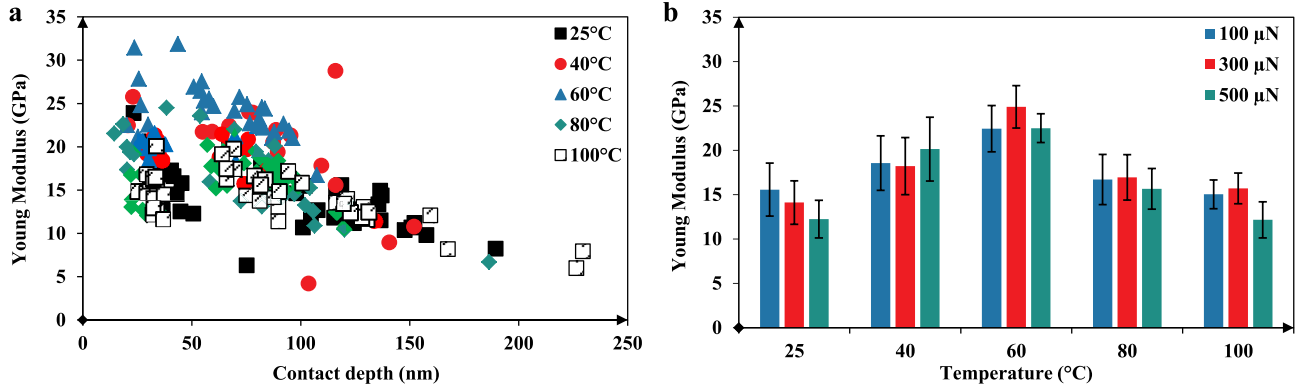


Fig. 8. Young's Modulus values obtained from nanoindentation of flax fibers at different sample temperatures, (a) with 500 μN of applied load, and (b) for different applied load values.

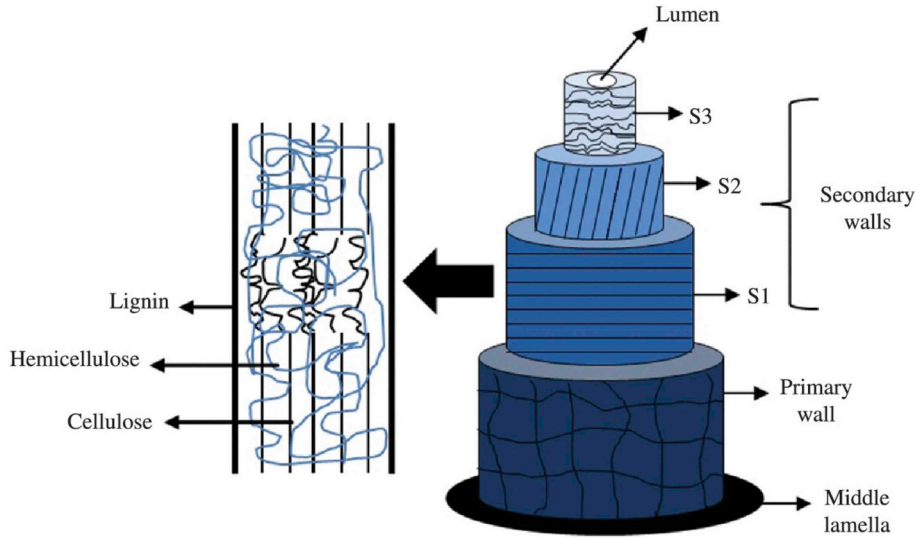


Fig. 9. Schematic illustration of flax elementary fiber and its chemical composition [32].

the change of the sliding speed. On the other side, the friction coefficient of flax fibers shows a different behavior depending on the sliding speed. Indeed, the friction coefficient of flax fibers decreases by heat increase at low sliding speed ($2\ \mu\text{m/s}$) as shown in Fig. 11(a). While increasing the sliding speed ($10\ \mu\text{m/s}$), the friction coefficient of flax fibers increases with rise in temperature ranging from $25\ ^\circ\text{C}$ to $60\ ^\circ\text{C}$ and decreases by heating the samples even further from $60\ ^\circ\text{C}$ to $100\ ^\circ\text{C}$ as shown in Fig. 11(b).

The microscopic friction behavior of PP matrix in this study is in good agreement with the sliding friction of PP reported in literature at macroscale by standard tribometers where the sliding friction of PP polymer decreases with temperature increase [36] which is due to the polymer softening that leads to the decrease of the tangential scratching force.

However, the microscopic friction behavior of flax fibers is influenced by the increase of the sliding speed. The friction behavior of flax fibers at low sliding speed ($2\ \mu\text{m/s}$) has the same trend as that of the PP matrix. At high sliding speed ($10\ \mu\text{m/s}$), the flax fibers friction seems to be affected by the thermo-mechanical behavior of flax fibers shown in Fig. 8(b) where increasing the fiber stiffness at the temperature range of $[25\ ^\circ\text{C}-60\ ^\circ\text{C}]$ increases the fiber friction and decreasing the fiber stiffness at the temperature range of $[60\ ^\circ\text{C}-100\ ^\circ\text{C}]$ decreases the fiber friction. This specific effect of sliding speed on the flax fiber's friction could be due to the time scale, which is important in the case of visco-elasto-plastic materials such as plant fibers [37]. Increasing the sliding speed increases the deformation rate when scratching which may

induce a visco-elastic contribution that is related to the thermo-mechanical behavior of flax fibers. In this context, the role of water release by heating could be significant since water molecules act as a plasticizer [34].

It is important to note that the micro-contact of the scratch could induce an additional thermal contribution on the contact zone. Indeed, the average temperature increase (ΔT) in the micro-contact is given by the following formula [38]:

$$\Delta T = 0.2 \times \frac{\mu \times E \times l \times V}{\lambda} \quad (1)$$

where μ is the friction coefficient, E is the elastic modulus, l is the root mean square of the height distribution, V is the sliding speed and λ is the thermal conductivity.

To keep this flash temperature (heat induced by friction) as low as possible for a contact between the diamond indenter and the bio-composite, and assuming that the parameter " l " has not a high variation at macroscale, the work-material should have a low elastic modulus and a high thermal conductivity. In the case of flax fibers and PP matrix, the elastic modulus of flax fibers is largely higher than that of PP matrix as shown in section 3.1. Moreover, the thermal conductivity of flax fibers (around $0.04\ \text{W/mK}$ [39–41]) is largely lower than that of PP matrix (around $0.2\ \text{W/mK}$ [42]). Therefore, the flash thermal contribution when scratching flax fibers is more important than that of scratching PP matrix, especially when increasing the sliding speed which increases more the heat induced by friction. This thermal phenomenon may

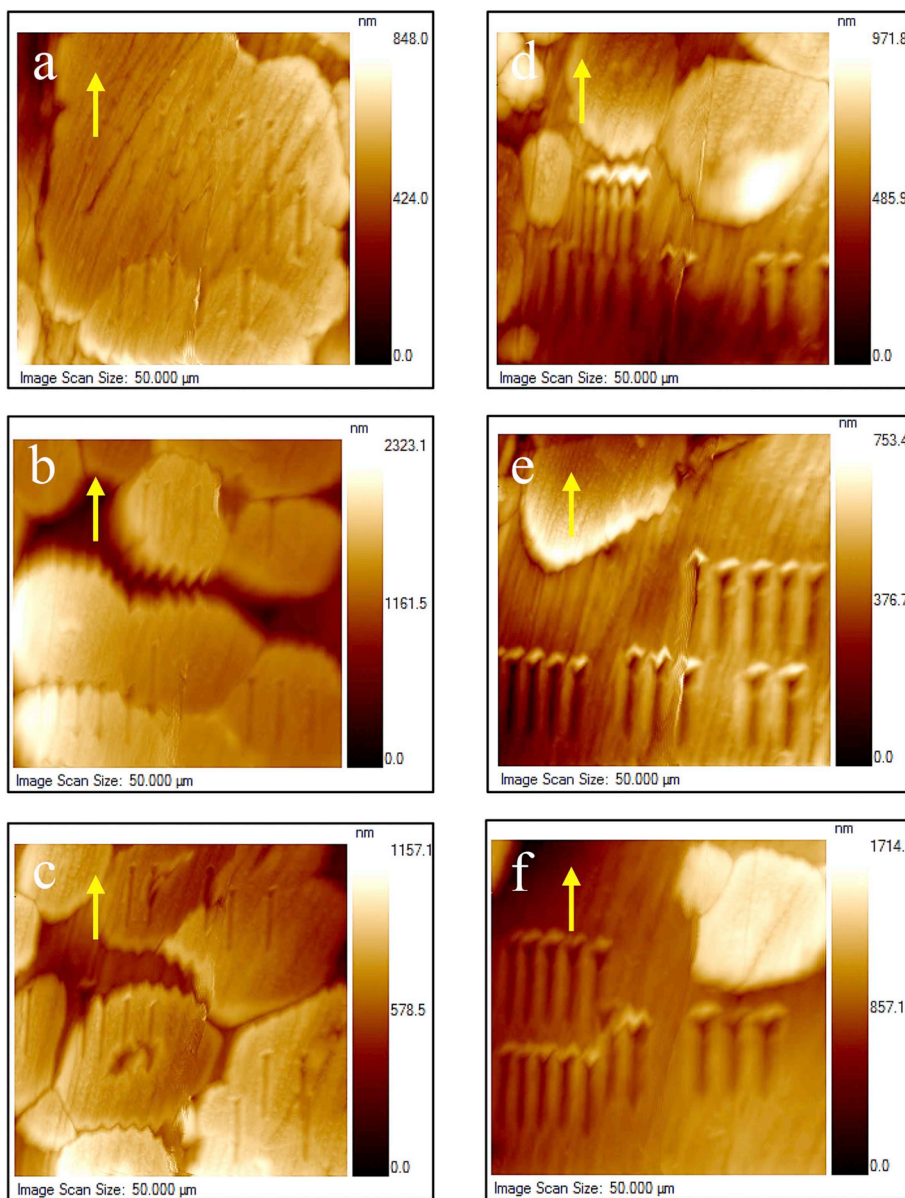


Fig. 10. Typical scanning probe images of scratching traces at $V = 10 \mu\text{m/s}$ on flax fibers (a,b,c) and PP matrix (d,e,f) at different temperatures. (a,d) $T = 25 \text{ }^\circ\text{C}$, (b,e) $T = 60 \text{ }^\circ\text{C}$ and (c,f) $T = 100 \text{ }^\circ\text{C}$. Yellow arrows show the scratching direction. (For interpretation of the references to colour in this figure legend, the reader is referred to the Web version of this article.)

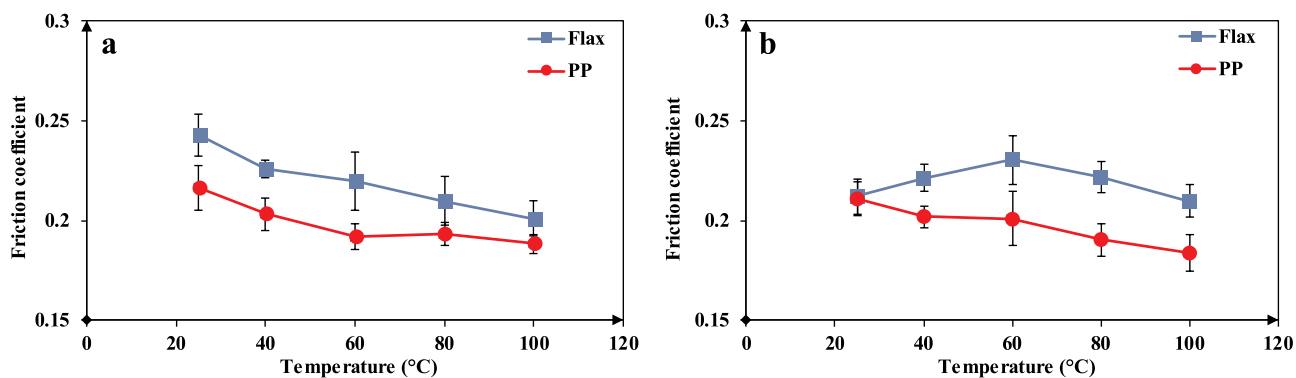


Fig. 11. Dynamic friction coefficient obtained by scratch-test of flax fibers and PP matrix for two siding speed values: (a) $2 \mu\text{m/s}$ and (b) $10 \mu\text{m/s}$.

contribute to the specific effect of sliding speed on the flax fiber's friction.

4. Conclusions

This paper deals with the thermal effect on the tribo-mechanical behavior of flax fiber reinforced polypropylene composites using nanoindentation and scratch-test experiments at different thermal conditions from room temperature (25 °C) to 100 °C. The following conclusions can be drawn:

- Increasing the NFRP sample temperature have not the same effect on the thermo-mechanical behavior of flax fibers and PP matrix:
 - Heating the composite sample in the considered temperature range decreases the stiffness of the PP matrix by increasing the material softening.
 - Heating the composite sample increases the stiffness of flax fibers in the temperature range of [25 °C–60 °C] and decreases it in the temperature range of [60 °C–100 °C]. The stiffness increase at the first heating step could be due to the water release inside elementary fibers while the stiffness decrease at the second heating step may be due to the softening of the amorphous structure of flax elementary fibers.
- Flax fibers induce higher friction than PP matrix regardless of the thermal conditions
- The friction coefficient of PP matrix decreases by temperature increase without significant influence of the sliding speed.
- The friction coefficient of flax fibers decreases by temperature increase at low sliding speed and behave similarly to the mechanical compartment at high sliding speed. The thermo-mechanical behavior of flax fibers affects their friction behavior at high sliding speed.

References

[1] Omrani EL, Menezes PK, Rohatgi P. State of the art on tribological behavior of polymer matrix composites reinforced with natural fibers in the green materials world. *Eng Sci Technol Int J* 2016;19:717–36. <https://doi.org/10.1016/J.JESTCH.2015.10.007>.

[2] Pickering KL, Aruan Efendy MG, Le TM. A review of recent developments in natural fibre composites and their mechanical performance. *Composites Part A Appl Sci Manuf* 2016;83:98–112. <https://doi.org/10.1016/J.COMPOSITESA.2015.08.038>.

[3] Shalwan A, Yousif BF. In State of Art: mechanical and tribological behaviour of polymeric composites based on natural fibres. *Mater Des* 2013;48:14–24. <https://doi.org/10.1016/j.matdes.2012.07.014>.

[4] Etaati A, Mehdizadeh SA, Wang H, Pather S. Vibration damping characteristics of short hemp fibre thermoplastic composites. *J Reinf Plast Compos* 2014;33:330–41. <https://doi.org/10.1177/0731684413512228>.

[5] Rajeshkumar G, Hariharan V. Free vibration characteristics of phoenix sp fiber reinforced polymer matrix composite beams. *Procedia Eng* 2014;97:687–93. <https://doi.org/10.1016/J.PROENG.2014.12.298>.

[6] Alves C, Ferrao PMC, Silva AJ, Reis LG, Freitas M, Rodrigues LB, et al. Ecodesign of automotive components making use of natural jute fiber composites. *J Clean Prod* 2010;18:313–27. <https://doi.org/10.1016/J.JCLEPRO.2009.10.022>.

[7] Shah DU. Developing plant fibre composites for structural applications by optimising composite parameters: a critical review. *J Mater Sci* 2013;48:6083–107. <https://doi.org/10.1007/s10853-013-7458-7>.

[8] Yousif BF, Lau STW, McWilliam S. Polyester composite based on betelnut fibre for tribological applications. *Tribol Int* 2010;43:503–11. <https://doi.org/10.1016/J.TRIBOINT.2009.08.006>.

[9] Nirmal U, Hashim J, Low KO. Adhesive wear and frictional performance of bamboo fibres reinforced epoxy composite. *Tribol Int* 2012;47:122–33. <https://doi.org/10.1016/j.triboint.2011.10.012>.

[10] Bakry M, Mousa MO, Ali WY. Friction and wear of friction composites reinforced by natural fibres. *Mater Werkst* 2013;44:21–8. <https://doi.org/10.1002/mawe.201300962>.

[11] Yallev TB, Kumar P, Singh I. Sliding wear properties of jute fabric reinforced polypropylene composites. *Procedia Eng* 2014;97:402–11. <https://doi.org/10.1016/J.PROENG.2014.12.264>.

[12] Nirmal U, Hashim J, Megat Ahmed MMH. A review on tribological performance of natural fibre polymeric composites. *Tribol Int* 2015;83:77–104. <https://doi.org/10.1016/J.TRIBOINT.2014.11.003>.

[13] Bajpai PK, Singh I, Madaan J. Tribological behavior of natural fiber reinforced PLA composites. *Wear* 2013;297:829–40. <https://doi.org/10.1016/J.WEAR.2012.10.019>.

[14] Davim JP, Reis P. Damage and dimensional precision on milling carbon fiber-

reinforced plastics using design experiments. *J Mater Process Technol* 2005;160:160–7. <https://doi.org/10.1016/j.jmatprotec.2004.06.003>.

[15] Abrate S, Walton D. Machining of composite materials. Part II: non-traditional methods. *Compos Manuf* 1992;3:85–94. [https://doi.org/10.1016/0956-7143\(92\)90120-J](https://doi.org/10.1016/0956-7143(92)90120-J).

[16] Baley C. Analysis of the flax fibres tensile behaviour and analysis of the tensile stiffness increase. *Compos Part A Appl Sci Manuf* 2002;33:939–48. [https://doi.org/10.1016/S1359-835X\(02\)00040-4](https://doi.org/10.1016/S1359-835X(02)00040-4).

[17] Chegiani F, Mezghani S, El Mansori M. On the multiscale tribological signatures of the tool helix angle in profile milling of woven flax fiber composites. *Tribol Int* 2016;100:132–40. <https://doi.org/10.1016/j.triboint.2015.12.014>.

[18] Chegiani F, Mezghani S, El Mansori M, Mkaddem A. Fiber type effect on tribological behavior when cutting natural fiber reinforced plastics. *Wear* 2015;332–333:772–9. <https://doi.org/10.1016/j.wear.2014.12.039>.

[19] Chegiani F, Mansori M El, El Mansori M. Mechanics of material removal when cutting natural fiber reinforced thermoplastic composites. *Polym Test* 2018;67:275–83. <https://doi.org/10.1016/j.polymertesting.2018.03.016>.

[20] Chegiani F, Mezghani S, El Mansori M. Correlation between mechanical scales and analysis scales of topographic signals under milling process of natural fibre composites. *J Compos Mater* 2016;51:2743–56. <https://doi.org/10.1177/0021998316676625>.

[21] Chegiani F, Mezghani S, El Mansori M. Experimental study of coated tools effects in dry cutting of natural fiber reinforced plastics. *Surf Coating Technol* 2015;284:264–72. <https://doi.org/10.1016/j.surfcoat.2015.06.083>.

[22] Chegiani F, El Mansori M, Mezghani S, Montagne A. Scale effect on tribo-mechanical behavior of vegetal fibers in reinforced bio-composite materials. *Compos Sci Technol* 2017;150:87–94. <https://doi.org/10.1016/j.compscitech.2017.07.012>.

[23] Chegiani F, Wang Z, El Mansori M, Bukkapatnam STS. Multiscale tribo-mechanical analysis of natural fiber composites for manufacturing applications. *Tribol Int* 2018;122:143–50. <https://doi.org/10.1016/j.triboint.2018.02.030>.

[24] Chegiani F, El Mansori M. Friction scale effect in drilling natural fiber composites. *Tribol Int* 2018;119:622–30. <https://doi.org/10.1016/j.triboint.2017.12.006>.

[25] El-Hofy MH, Soo SL, Aspinwall DK, Sim WM, Pearson D, M'Saoubi R, et al. Tool temperature in slotting of CFRP composites. *Procedia Manuf* 2017;10:371–81. <https://doi.org/10.1016/J.PROMFG.2017.07.007>.

[26] Weinert K, Kempmann C. Cutting temperatures and their effects on the machining behaviour in drilling reinforced plastic composites. *Adv Eng Mater* 2004;6:684–9. <https://doi.org/10.1002/adem.200400025>.

[27] Hangen U, Chen C-L, Richter A. Mechanical characterization of PM2000 oxide-dispersion-strengthened alloy by high temperature nanoindentation. *Adv Eng Mater* 2015;17:1683–90. <https://doi.org/10.1002/adem.201500095>.

[28] Drozdov AD. Effect of temperature on the viscoelastic and viscoplastic behavior of polypropylene. *Mech Time-Dependent Mater* 2010;14:411–34. <https://doi.org/10.1007/s11043-010-9118-5>.

[29] Tripathi D. *Practical guide to polypropylene*. Shropshire, UK: Rapra Technology LTD; 2002.

[30] Van de Velde K, Kiekens P. Thermoplastic polymers: overview of several properties and their consequences in flax fibre reinforced composites. *Polym Test* 2001;20:885–93. [https://doi.org/10.1016/S0142-9418\(01\)00017-4](https://doi.org/10.1016/S0142-9418(01)00017-4).

[31] Kannan TG, Wu CM, Cheng KB, Wang CY. Effect of reinforcement on the mechanical and thermal properties of flax/polypropylene interwoven fabric composites. *J Ind Text* 2013;42:417–33. <https://doi.org/10.1177/1528083712442695>.

[32] Pereira PHF, Rosa M de F, Cioffi MOH, Benini KCC de C, Milanese AC, Voorwald HJC, et al. Vegetal fibers in polymeric composites: a review. *Polímeros* 2015;25:9–22. <https://doi.org/10.1590/0104-1428.1722>.

[33] Dittenber DB, GangaRao HVS. Critical review of recent publications on use of natural composites in infrastructure. *Composites Part A Appl Sci Manuf* 2012;43:1419–29. <https://doi.org/10.1016/j.compositesa.2011.11.019>.

[34] Hon D N-S, Shiraishi N. *Wood and cellulosic chemistry*. New York: Marcel Dek.; 2000.

[35] Kong L, Zhao Z, He Z, Yi S. Effects of steaming treatment on crystallinity and glass transition temperature of *Eucalyptus grandis* × *E. urophylla*. *Results Phys* 2017;7:914–9. <https://doi.org/10.1016/J.RINP.2017.02.017>.

[36] Ludema KC, Tabor D. The friction and visco-elastic properties of polymeric solids. *Wear* 1966;9:329–48. [https://doi.org/10.1016/0043-1648\(66\)90018-4](https://doi.org/10.1016/0043-1648(66)90018-4).

[37] Richard F, Poilâne C, Yang H, Gehring F, Renner E. A viscoelastoplastic stiffening model for plant fibre unidirectional reinforced composite behaviour under monotonic and cyclic tensile loading. *Compos Sci Technol* 2018;167:396–403. <https://doi.org/10.1016/J.COMPOSITECH.2018.08.020>.

[38] Popov V L. *Contact mechanics and Friction: physical principles and applications*. Heidelberg: Springer Berlin Heidelberg; 2009. <https://doi.org/10.1007/978-3-642-10803-7>.

[39] Sutton A, Black D, Walker P. *Natural fibre insulation: an introduction to low-impact building materials*. BRE Electron Publ; 2011.

[40] Stapulionienė R, Vaitkus S, Vėjelis S, Sankauskaitė A. Investigation of thermal conductivity of natural fibres processed by different mechanical methods. *Int J Precis Eng Manuf* 2016;17:1371–81. <https://doi.org/10.1007/s12541-016-0163-0>.

[41] Kymäläinen H-R, Sjöberg A-M. Flax and hemp fibres as raw materials for thermal insulations. *Build Environ* 2008;43:1261–9. <https://doi.org/10.1016/J.BUILDENV.2007.03.006>.

[42] Chen L, Xu H-F, He S-J, Du Y-H, Yu N-J, Du X-Z, et al. Thermal conductivity performance of polypropylene composites filled with polydopamine-functionalized hexagonal boron nitride. *PLoS One* 2017;12:e0170523. <https://doi.org/10.1371/journal.pone.0170523>.